THE JOURNAL OF BIOLOGICAL CHEMISTRY VOL. 291, NO. 27, pp. 13964–13973, July 1, 2016

Natural Product Anacardic Acid from Cashew Nut Shells Stimulates Neutrophil Extracellular Trap Production and Bactericidal Activity*[S]

Received for publication, October 1, 2015, and in revised form, May 7, 2016 Published, JBC Papers in Press, May 13, 2016, DOI 10.1074/jbc.M115.695866

Andrew Hollands[‡1], Ross Corriden[§1], Gabriela Gysler[‡], Samira Dahesh[‡], Joshua Olson[‡], Syed Raza Ali[‡], Maya T. Kunkel[§], Ann E. Lin[‡], Stefano Forli[¶], Alexandra C. Newton[§], Geetha B. Kumar[‖], Bipin G. Nair[‖], J. Jefferson P. Perry[‖], and Victor Nizet[‡ ‡‡2]**

*From the Departments of [‡]Pediatrics and [§]Pharmacology and the [‡‡]Skaggs School of Pharmacy and Pharmaceutical Sciences, University of California, San Diego, La Jolla, California 92093, the [¶]Department of Integrative Structural and Computational Biology, Scripps Research Institute, La Jolla, California 92037, the [‖]School of Biotechnology, Amrita University, Kollam, 690525 Kerala, India, and the **Department of Biochemistry, University of California, Riverside, California 92521*

Emerging antibiotic resistance among pathogenic bacteria is an issue of great clinical importance, and new approaches to therapy are urgently needed. Anacardic acid, the primary active component of cashew nut shell extract, is a natural product used in the treatment of a variety of medical conditions, including infectious abscesses. Here, we investigate the effects of this natural product on the function of human neutrophils. We find that anacardic acid stimulates the production of reactive oxygen species and neutrophil extracellular traps, two mechanisms utilized by neutrophils to kill invading bacteria. Molecular modeling and pharmacological inhibitor studies suggest anacardic acid stimulation of neutrophils occurs in a PI3K-dependent manner through activation of surface-expressed G protein-coupled sphingosine-1-phosphate receptors. Neutrophil extracellular traps produced in response to anacardic acid are bactericidal and complement select direct antimicrobial activities of the compound.

The rapid increase in multidrug-resistant bacterial strains is a problem of great concern to the medical and public health communities. Currently, the emergence of antibiotic resistance outpaces the development of antibiotic compounds (1), stimulating interest in novel approaches to treat difficult infections. Therapies that enhance the bactericidal activity of host immune cells (*e.g.* neutrophils) represent one such alternative.

Natural products have garnered substantial interest as lead points for identification of new pharmaceutical agents (2). Leaves or nut shell extracts from *Anacardium occidentale*, commonly known as the cashew tree, have long been used to treat inflammation and other conditions, including asthma, ulcers, and cancer (3). Although the efficacy of these compounds for treating such disorders has not been established in controlled trials, the major component of cashew nut shell extract, anacardic acid, has been shown to exert a variety of effects on both prokaryotic and eukaryotic cells (4, 5).

Anacardic acid is a blanket term applied to a family of closely related compounds consisting of salicylic acid with a 15-carbon alkyl chain, which exist either in a fully saturated form or as a monoene, diene, or triene. Anacardic acid has been shown to exhibit direct antimicrobial activity against a number of bacterial species, including *Propionibacterium acnes*, *Staphylococcus aureus*, and *Helicobacter pylori* (4, 6, 7). However, it is perhaps best known as an inhibitor of eukaryotic histone acetyltransferase (8) that has been shown to inhibit NFκB activities (9) and, more recently, matrix metalloproteinase activity (10). Through these mechanisms, anacardic acid may induce autophagy (11) and enhance apoptosis (12) of mammalian cells. It has been proposed that the potentiation of apoptosis by anacardic acid results from inhibition of genes involved in cell survival and proliferation (9). Although anacardic acid has antioxidant properties *in vitro* (13, 14), it may also stimulate cellular superoxide production by inhibiting the SUMOylation of NADPH oxidase (15). Given the importance of these pathways in the regulation of neutrophil function and innate immune activities, we investigated the actions of anacardic acid on human neutrophils, with an emphasis on the formation of neutrophil extracellular traps (NETs),[3] reactive oxygen species (ROS)-dependent, DNA-based structures coated with antimicrobial compounds that entrap and kill pathogens (16).

Results

Antimicrobial Activity of Anacardic Acid—We assessed the ability of anacardic acid, either in a commercial fully saturated form or in its natural cashew nut shell extracted form, to directly kill bacteria. Cashew nut shell-extracted anacardic acid, a mixture of fully saturated, monoene, diene, and triene forms of anacardic acid, exhibited antimicrobial activity against

* This work was supported by National Institutes of Health Grants AI057153, HD71600, GM43154, AR059968, and AI124316 and by funds from Amrita Vishwa Vidyapeetham University. The authors declare that they have no conflicts of interest with the contents of this article. The content is solely the responsibility of the authors and does not necessarily represent the official views of the National Institutes of Health.

[S] This article contains supplemental Table S1 and supplemental Fig. S1.

[1] Both authors contributed equally to this work.

[2] To whom correspondence should be addressed: School of Medicine, University of California, San Diego, La Jolla, CA 92093-0760. Tel.: 858-534-7408; Fax: 858-246-1868; E-mail: vnizet@ucsd.edu.

[3] The abbreviations used are: NET, neutrophil extracellular trap; ROS, reactive oxygen species; S1P, sphingosine-1-phosphate; S1PR, S1P receptor; MRSA, methicillin-resistant *S. aureus*; DPI, diphenyleneiodonium; PMA, phorbol 12-myristate 13-acetate; CNSE, cashew nut shell-extracted; HBSS, Hanks' balanced salt solution.

TABLE 1
Minimum inhibitory concentration of anacardic acid against selected bacterial species

Bacterial species and strain tested	Commercial fully saturated anacardic acid	Cashew nut shell extract anacardic acid
	μM	μM
S. aureus (USA300-TCH1516) methicillin-resistant	>80	20
S. pyogenes (M49-NZ131)	5	5
S. agalactiae (serotype III-COH1)	5	5
E. coli (K12-DH5α)	>80	>80
P. aeruginosa (PA01)	>80	>80

three different Gram-positive bacterial species tested (MRSA, *Staphylococcus pyogenes*, and *Staphylococcus agalactiae*), but not against the two Gram-negative bacterial species tested (*Escherichia coli* and *Pseudomonas aeruginosa*) (Table 1). Commercial fully saturated anacardic acid was also ineffective at killing the Gram-negative bacterial test species but, despite showing antimicrobial activity against *S. pyogenes* and *S. agalactiae*, did not kill MRSA. In kinetic killing assays, anacardic acid was found to slow the growth of Gram-positive bacteria down to the lowest concentration tested, one-eighth of the minimum inhibitory concentration (Fig. 1).

Anacardic Acid Stimulates Neutrophil Oxidative Burst—Oxidative burst was used as an initial indicator of neutrophil activation. The addition of anacardic acid to freshly isolated human neutrophils stimulated production of ROS over time (Fig. 2*A*) and in a concentration-dependent manner (Fig. 2*B*). Induction of neutrophil ROS production was similar in response to commercial anacardic acid or anacardic acid extracted from cashew nut shells (Fig. 2*C*). Oxidative burst stimulation by anacardic acid was validated by quenching ROS with the NADPH oxidase inhibitor diphenyleneiodonium (DPI; Fig. 2*D*) and assessing ROS production via a flow cytometry-based assay (Fig. 2*E*). No induction of ROS was observed in response to salicylic acid, the core structure of anacardic acid, revealing that the alkyl chain of anacardic acid is required for activation of the neutrophil oxidative burst (Fig. 2*F*).

Anacardic Selectively Stimulates Specific Neutrophil Pro-inflammatory Pathways—Unlike PMA, accumulation of extracellular ROS was not observed upon anacardic acid treatment in a lucigenin-based extracellular ROS assay (Fig. 3*A*). Furthermore, neutrophil degranulation was not observed in response to anacardic acid treatment, suggesting that anacardic acid does not trigger a general activation of neutrophils (Fig. 3*B*). Immunocytochemical analysis revealed increased intracellular gp91^{phox} levels in anacardic acid-treated neutrophils (Fig. 3*C*), but no significant release of the antimicrobial peptide LL-37 was detected (Fig. 3*D*). Finally, although anacardic acid is known to be a potential SUMOylation inhibitor (15), under the conditions of these assays, no inhibition of SUMOylation was observed (Fig. 3*E*).

Neutrophil Extracellular Trap Formation—Oxidative burst in neutrophils may precede the formation of NETs. We found that stimulation of neutrophils with anacardic acid not only triggered ROS production but also led to NET production (Fig. 4*A*). NET induction by anacardic was concentration-dependent (Fig. 4*B*), and addition of the NADPH oxidase inhibitor DPI blocked anacardic acid-induced NET formation (Fig. 4*C*). Although anacardic acid elicits a similar phenotype of ROS induction and NET formation as phorbol 12-myristate 13-acetate (PMA), a known PKC activator, anacardic acid treatment does not boost neutrophil PKC activity (Fig. 4*D*).

Anacardic Acid Mimics Sphigosine-1-phosphate—To identify possible targets for anacardic acid on neutrophils, we utilized the similarity ensemble approach, an *in silico* platform that relates proteins based on the set-wise chemical similarity among their ligands (17). Several members of the sphingosine-1-phosphate receptor (S1PR) family of G protein-coupled receptors were found to be possible targets (supplemental Table S1). *In silico* docking confirmed that anacardic acid may bind to this family of receptors, with anacardic acid predicted to bind to the S1P1 crystal structure (Protein Data Bank code 3V2Y) at −8.09 kcal/mol. Predicted binding mode shows that the salicylic acid group of anacardic acid can establish hydrogen bonds with S1P1 residues Tyr^{29}, Lys^{34}, and Arg^{120}, in a similar fashion to the phosphate group of sphingolipid mimic ML5 present in the crystal structure, wherein the pentadecyl aliphatic chain fills the large hydrophobic pocket, overlapping closely with the hydrophobic component of ML5 (Fig. 5*A*). The Tyr^{29}, Lys^{34}, and Arg^{120} residues are localized in highly conserved regions; amino acids Tyr^{29} and Arg^{120} are identical in the S1P1 and S1P4 receptors, whereas Lys^{34} is instead an arginine in S1PR4 (supplemental Fig. S1), suggesting that K34R should be capable of establishing the key hydrogen bond shown in Fig. 5*A*. Oxidative burst was blocked by CYM50358 hydrochloride, a S1PR4-selective antagonist but not VPC23019, a S1PR1 and S1PR3 antagonist, suggesting a critical role for S1PR4 in anacardic acid stimulation of neutrophils (Fig. 5*B*). Nearly complete (~85%) and concentration-dependent inhibition of neutrophil activation by anacardic acid was observed using the CYM50358 hydrochloride inhibitor (Fig. 5*C*).

Anacardic Acid Acts through PI3K—Multiple signaling pathways have been implicated in neutrophil oxidative burst and NET production. Likewise, S1P receptors have also been linked to numerous signaling pathways. To assess the mechanism by which anacardic acid stimulates neutrophils, we tested a select panel of kinase inhibitors. We found that neutrophil stimulation by anacardic acid was blocked by inhibiting PI3K, but not by inhibiting Src tyrosine kinase or MEK (Fig. 6*A*). Consistent with this finding, an assessment of total/phospho-Akt and ERK revealed a significant increase in Akt phosphorylation in anacardic acid-treated neutrophils *versus* untreated controls (Fig. 6*B*). The dependence of anacardic acid-induced oxidative burst on PI3K was further confirmed in an assay using the PI3K inhibitor wortmannin, which significantly inhibited anacardic acid-induced increase in ROS (Fig. 6*C*).

Bacterial Killing by Neutrophils Is Enhanced by Anacardic Acid—We used a NET-biased killing assay to determine the bactericidal capacity of NETs stimulated by anacardic acid,

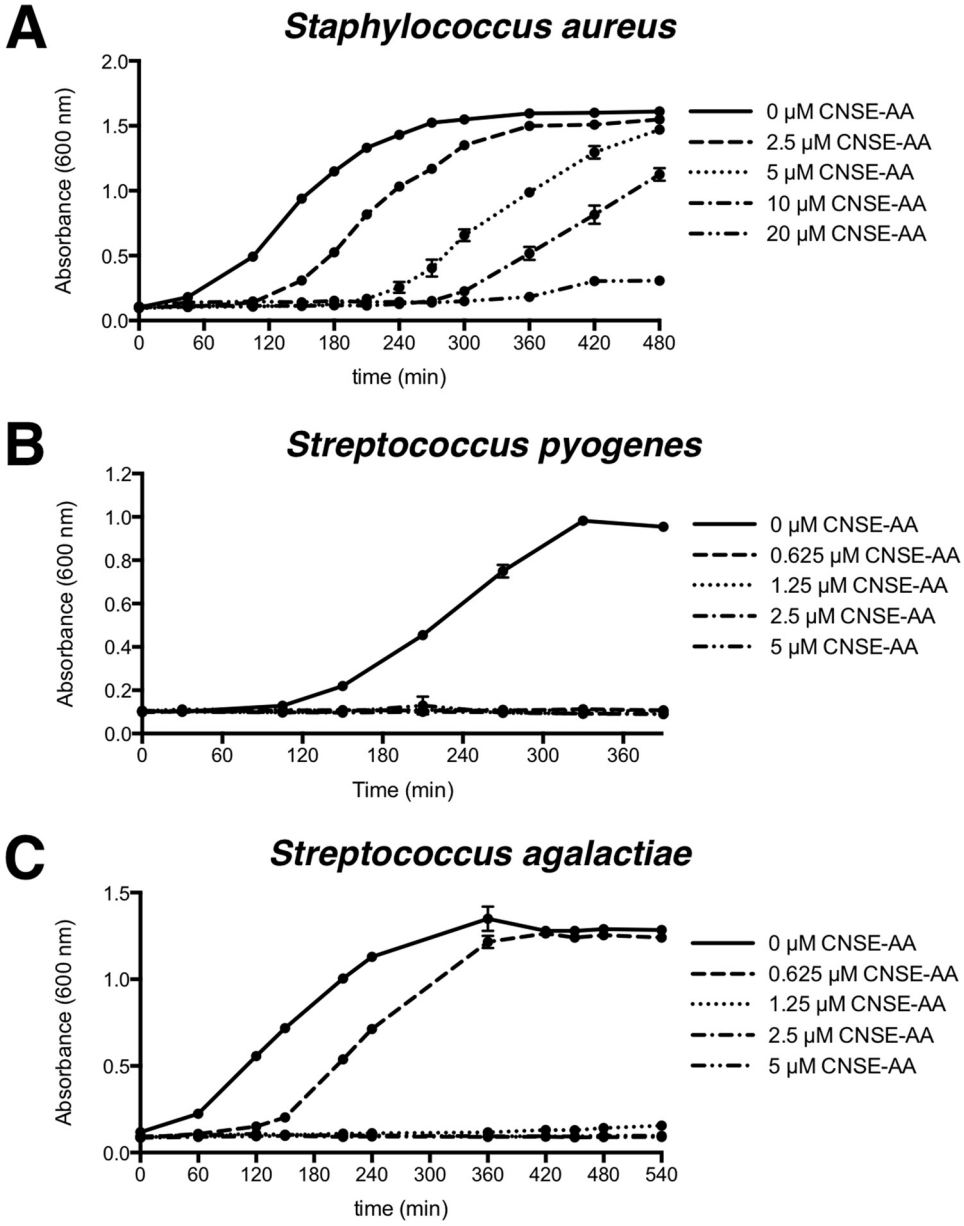

FIGURE 1. **Anacardic acid inhibits bacterial growth.** Growth of bacteria over time in the presence of a range of concentrations of cashew nut shell-extracted anacardic acid. The data shown are expressed as mean values ± S.D. ($n = 3$). The experiments were performed three times, and a representative experiment is shown. *A*, *S. aureus*. *B*, *S. pyogenes*. *C*, *S. agalactiae*.

finding that such NETs were capable of killing USA300 MRSA (Fig. 7*A*), group A *Streptococcus* (Fig. 7*B*), and *E. coli* (Fig. 7*C*). In these figures, survival is presented as a percentage of compound-only control groups (*e.g.* without neutrophils). Notably, DNase almost completely reversed anacardic acid-mediated neutrophil killing of MRSA, whereas cytochalasin D had no significant effect, suggesting that such killing occurs primarily through NETs. Confocal microscopy and SYTO green/propidium iodide costaining revealed dead bacteria entrapped in NET structures stimulated by anacardic acid (Fig. 7*D*).

Discussion

Anacardic acid has long been used as a therapeutic agent in herbal medicine; although the molecular mechanisms underlying its activity are still poorly understood, its ability to modulate superoxide formation led us to investigate its effects on innate immune function and bacterial clearance. In addition to exhibiting direct antimicrobial effects against a series of important human Gram-positive pathogens, we found that anacardic acid enhanced neutrophil antibacterial function by promoting extracellular trap production. NETs are DNA-based structures that have been shown to play key role in pathogen clearance by neutrophils (18, 19). We show that anacardic acid-induced NETs are capable of ensnaring and killing bacteria, which likely contributes to enhanced bactericidal activity of anacardic acid-treated neutrophils *in vitro*.

Using computation approaches and known crystal structures, we identified the G protein-coupled sphingosine-1-phosphate receptors as likely targets of anacardic acid. This complements our previous finding that sphigosine-1-phos-

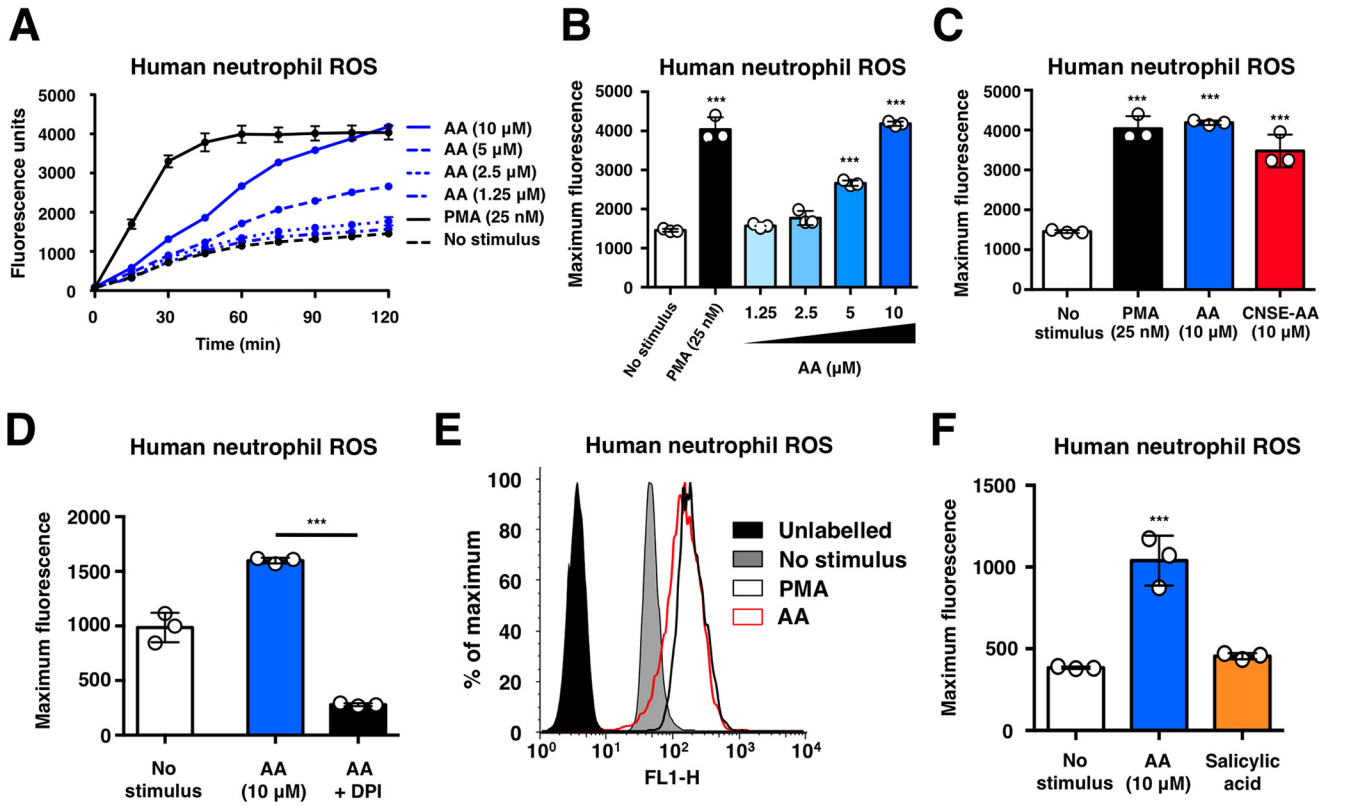

FIGURE 2. **Anacardic acid stimulates neutrophil oxidative burst.** *A*, ROS production by human neutrophils stimulated with anacardic acid ($n = 3$). *B*, total ROS generation by human neutrophils in the presence of anacardic acid ($n = 3$). *C*, ROS generation by human neutrophils stimulated with commercial anacardic acid (*AA*) or CNSE anacardic acid ($n = 3$). *D*, ROS generation in response to anacardic acid and inhibited with DPI (10 μM) ($n = 3$). *E*, quantification of ROS generation by flow cytometry of human neutrophils (histogram shown is a representative plot based on the results of three independent experiments). *F*, ROS generation by human neutrophils stimulated with anacardic acid or salicylic acid ($n = 3$). Assays were performed at least three times, and a representative experiment is shown; unless otherwise noted, the data are expressed as mean values ± S.D. Where applicable, the results were analyzed by one-way analysis of variance and post hoc Newman Keuls test. ***, $p < 0.001$ *versus* control values.

phate-related compounds, such as ceramide, can induce NET production in human neutrophils (20). We found that the S1P4-selective antagonist CYM 50358 (21), but not an antagonist of the S1P1/S1P3 receptors, was a potent inhibitor of anacardic acid-induced ROS production. The S1P4 receptor is predominantly expressed by immune cells, including neutrophils (22); intriguingly, previous work has shown that mice deficient in S1P lyase, an enzyme that catalyzes degradation of S1P, exhibit features of an inflammatory response that is ameliorated by deletion of the S1P4 receptor (23).

Consistent with investigations using other pharmacological agents to stimulate NET production (19, 24), we found anacardic acid-induced NET production to be both ROS- and PI3K-dependent; this is in keeping with reports describing coupling of the S1P4 receptor to $G\alpha_{12/13}$ (25), which has been shown to trigger cell death pathways via activation of PI3K (26). Given the diverse array of GPCRs acting through $G\alpha_{12/13}$, our findings could help guide future efforts to identify novel and potentially more selective/potent, immune-boosting compounds.

Natural products, such as anacardic acid, represent an important resource for drug discovery efforts and can yield not only potential therapeutic agents but also scaffolds on which to develop more potent and efficacious drugs. Our findings reveal a role of the S1P4 receptor as a mediator of NET production and identify anacardic acid as a potential lead compound to boost neutrophil function in innate immune defense.

Experimental Procedures

Materials—Commercial, fully saturated anacardic acid was obtained from Cayman Chemicals (Ann Arbor, MI). Cashew nut shell-extracted (CNSE) anacardic acid was purified as previously described (10); the same preparation of CNSE anacardic acid was used in this study. CYM50358 and VPC23019 were obtained from Tocris Bioscience (Bristol, UK). Unless otherwise noted, all other compounds were purchased from Sigma-Aldrich.

Bacterial Strains—*E. coli* (strain K12-DH5α), methicillin-resistant *S. aureus* (strain USA300-TCH1516), *P. aeruginosa* (strain PAO1), *S. pyogenes* (strain M49-NZ131), and *S. agalactiae* (strain COH1) were used in this study.

Neutrophil Isolation—Human venous blood was drawn from healthy volunteers, with heparin added as an anticoagulant, according to a protocol approved by the local ethics committee. Polymorphprep (Axis Shield, Dundee, Scotland) was used to isolate neutrophils according to the manufacturer's instructions. In brief, 20 ml of blood was layered on an equal volume of Polymorphprep in 50-ml conical tubes; after centrifugation for 30 min at 600 × *g* (24 °C, no brakes), the neutrophil layer was collected, resuspended in PBS in a fresh tube, and pelleted via centrifugation at 400 × *g* (24 °C, no brakes). Supernatant was aspirated, and cell pellets were gently resuspended prior to addition of 5 ml of TC grade H_2O (with gentle mixing) to lyse

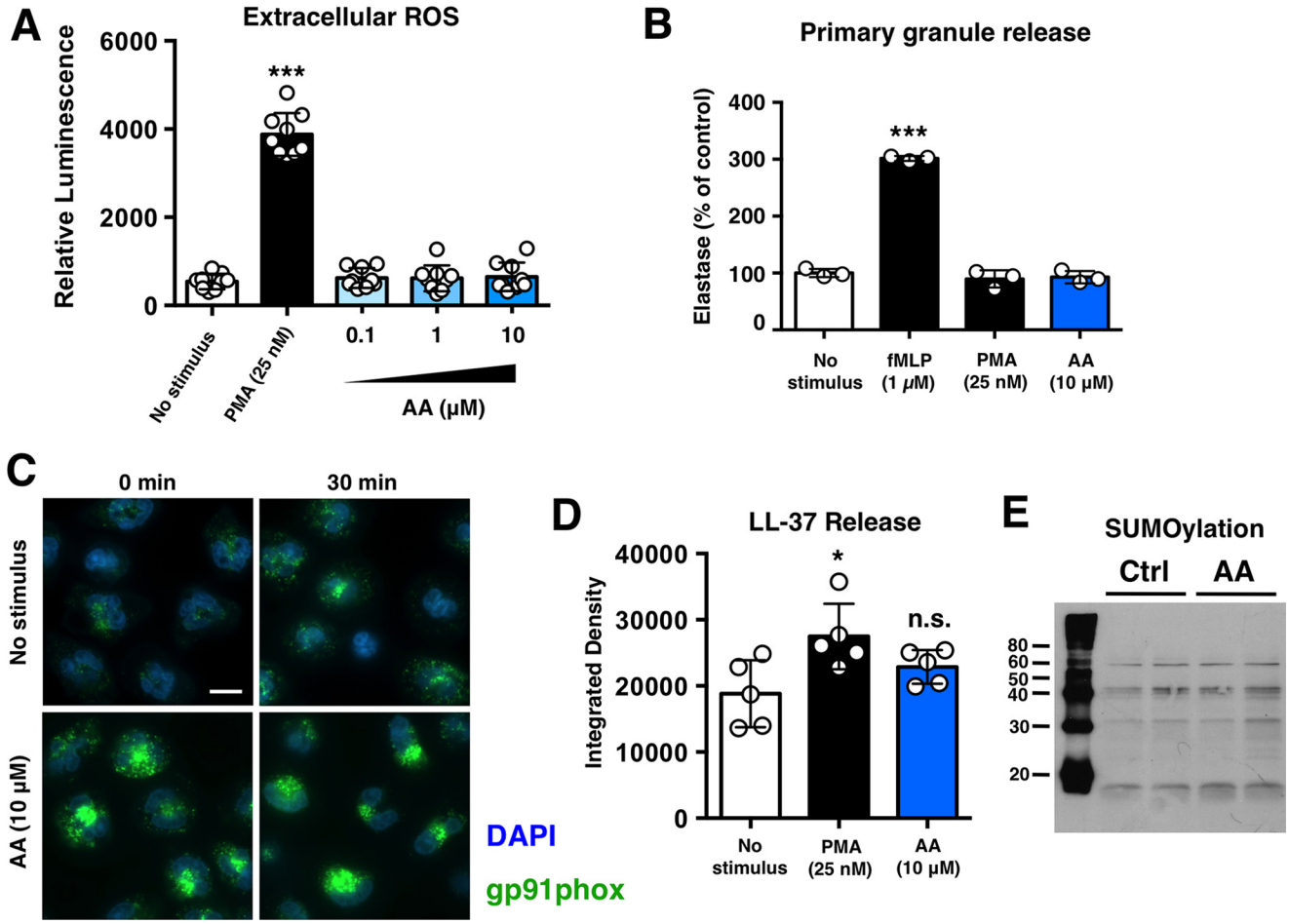

FIGURE 3. **Anacardic selectively stimulates specific neutrophil pro-inflammatory pathways.** *A*, lucigenin-based assay to assess extracellular ROS levels following stimulation with anacardic acid (*AA*) or PMA ($n = 9$). *B*, assessment of neutrophil degranulation/elastase release using the colorimetric elastase substrate *N*-methoxysuccinyl-Ala-Ala-Pro-Val-*p*-nitroanilide. *fMLP*, *N*-formyl-Met-Leu-Phe. *C*, immunocytochemical analysis of gp91^{phox} (*green*) in control and anacardic-acid treated neutrophils. Cell nuclei are stained with Hoerscht 33342 (*blue*). The *scale bar* represents 10 μm. *D*, dot-blot based assessment of LL-37 release from control, anacardic acid-treated, and PMA-treated neutrophils ($n = 5$). Anacardic acid does not stimulate neutrophil degranulation. *E*, anacardic acid does not inhibit SUMOylation in neutrophils (molecular masses shown are in kDa). Unless otherwise noted, data shown are expressed as mean values ± S.D. and are representative of at least three independent experiments performed in triplicate. Where applicable, the results were analyzed by one-way analysis of variance and post hoc Newman Keuls test. **, $p < 0.01$; ***, $p < 0.001$ *versus* control values. *Ctrl*, control.

erythrocytes. After 30 s, 45 ml of PBS was added, and the cells were centrifuged at 400 × *g* (24 °C, no brakes). Neutrophil pellets were gently resuspended in 1 ml of PBS, counted, and kept at room temperature at a concentration of 1×10^7 cells/ml until used in experiments.

Minimum Inhibitory Concentration Assays—To assess antimicrobial activity of anacardic acid in solution, bacteria were first grown in sterile Todd Hewitt broth to early log phase (A_{600} = 0.1). Bacterial suspensions (50 μl) were then distributed in 96-well plates and 2-fold serial dilutions of anacardic acid (either commercial or CNSE) were added. Absorbance at 600 nm was measured before and after overnight incubation at 37 °C, and minimum inhibitory concentration values were determined based on the ability of compounds to inhibit bacterial proliferation by at least 80%.

Bacterial Growth Curves—Glass tubes containing Todd Hewitt broth with or without anacardic acid or CNSE anacardic acid were inoculated with a sufficient volume of overnight bacterial culture to yield an optical density (600 nm) = 0.1. Cultures were incubated at 37 °C (with shaking), and optical density was monitored over time with a Spectronic 20D+ spectrophotometer (Thermo Scientific, Waltham, MA) to assess bacterial growth rates.

NET Quantification—Neutrophils were resuspended in HBSS (with Ca^{2+}/Mg^{2+}) at a concentration of 2×10^6 cells/ml and added to 96-well plates (2×10^5 cells/well). HBSS and various concentrations of either anacardic acid or CNSE anacardic acid were added to applicable wells to a final volume of 200 μl. Following 2 h of incubation at 37 °C with 5% CO_2, 50 milliunits of micrococcal nuclease (in a volume of 50 μl) was added to each well. After 10 min of incubation at 37 °C, EDTA was added to each well (final concentration, 5 mM) to stop the nuclease reaction. The plates were then centrifuged for 8 min at 200 × *g*, and 100-μl supernatant samples were collected and transferred to a flat-bottomed 96-well assay plate. DNA was quantified using PicoGreen DNA dye (Life Technologies) and a SpectraMax M3 plate reader (Molecular Devices) as per the manufacturers' instructions.

NET Visualization—NET production was stimulated with anacardic acid or CNSE anacardic acid in 96-well plates as

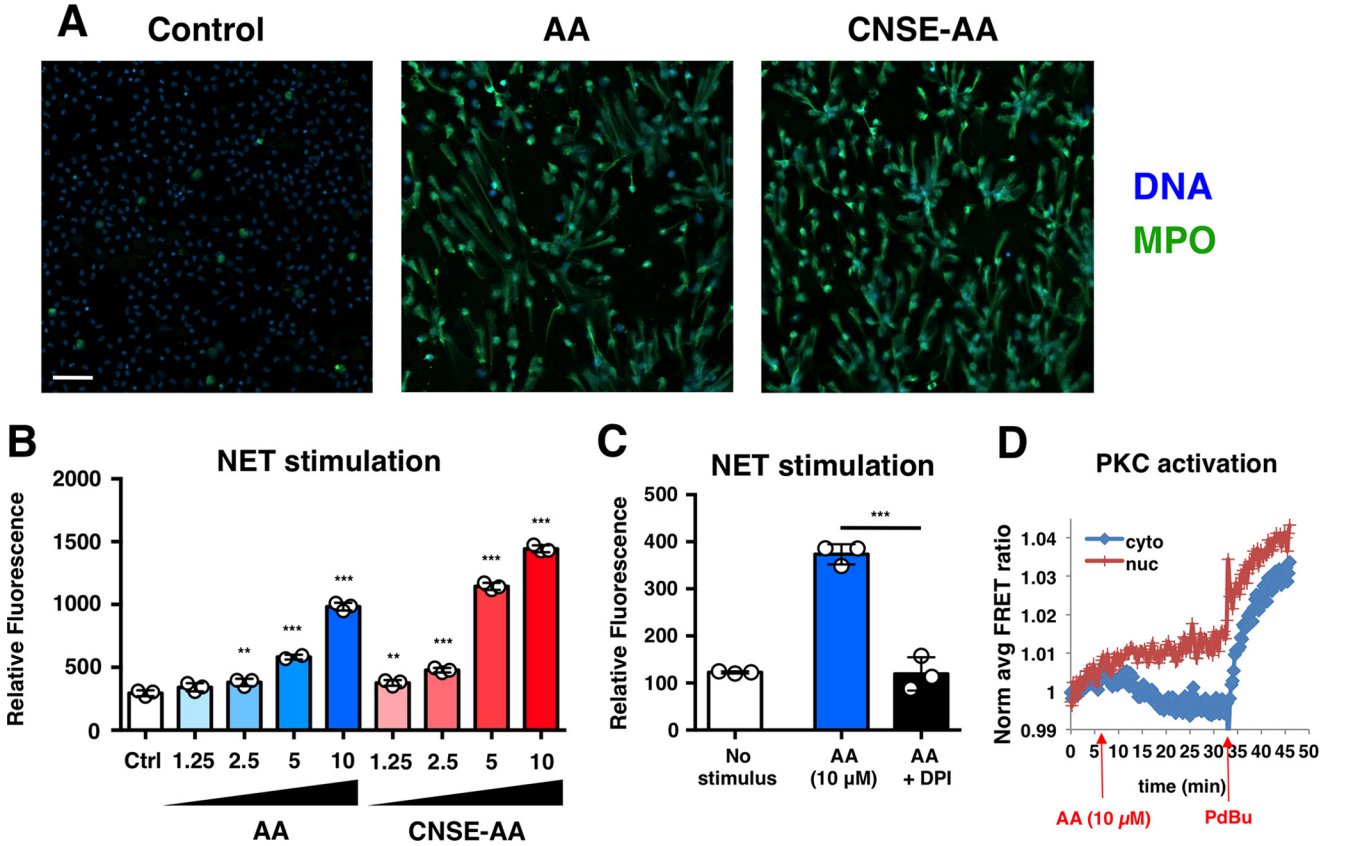

FIGURE 4. **Anacardic acid stimulates NETs.** *A*, immunocytochemical staining of extracellular DNA structures produced by neutrophils stimulated with commercial anacardic acid (*AA*; 10 μM) or CNSA anacardic acid (10 μM). The *scale bar* represents 50 μm. *MPO*, myeloperoxidase. *B*, quantification of NETs produced by human neutrophils stimulated with anacardic acid. *C*, quantification of NETs by human neutrophils stimulated with anacardic acid and inhibited with DPI (10 μM). *D*, HeLa cells transfected with CKAR, a FRET-based reporter for PKC-mediated phosphorylation, were treated with anacardic acid (10 μM) and phorbol 12,13-dibutyrate (*PdBu*; 200 nM) to assess PKC activation. The data shown are expressed as mean values ± S.D. and a representative experiment is shown of three independent experiments performed in triplicate. Where applicable, the results were analyzed by one-way analysis of variance and post hoc Newman Keuls test. **, $p < 0.01$; ***, $p < 0.001$ *versus* control values. *Ctrl*, control.

described above. After 2 h of incubation at 37 °C with 5% CO_2, the cells were fixed by addition of 16% paraformaldehyde (4% final concentration; 30 min incubation at room temperature). After blocking for 45 min with PBS containing 2% bovine serum albumin (2% PBS-BSA) and 2% goat serum, the cells were incubated for 1 h with rabbit anti-human myeloperoxidase primary antibody (1:300 in 2% PBS-BSA; Dako North America, Inc., Carpinteria, CA; product no. A0398) and 45 min (protected from light) with Alexa Fluor 488 goat anti-rabbit IgG secondary antibody (1:500 in 2% BSA-PBS; Life Technologies). The cells were then incubated with 1 μM DAPI for 10 min. The cells were washed three times with PBS after each staining step, all performed at room temperature. The images were obtained using a Zeiss AxioObserver D1 microscope equipped with an LD A-Plan 20×/0.35 Ph1 objective.

Live/Dead Staining of Bacteria—Neutrophils were plated on glass coverslips in 24-well plates at a density of 2×10^5 cells/well, and NET production was stimulated by adding 10 μM anacardic acid and incubating at 37 °C with 5% CO_2 for 2 h. In parallel, *S. aureus* bacteria were stained using a LIVE/DEAD BacLight kit (Life Technologies) as per the manufacturer's instructions; after stimulation of NET production, bacteria were added to wells containing neutrophils at an multiplicity of infection of 10 and spun at 1600 rpm for 10 min. To assess the presence of live/dead bacteria in NETs, images were captured using an Olympus FV1000 confocal microscope equipped with a 63× objective.

Reactive Oxygen Species Production Assay—Neutrophils (1×10^6 cells/ml) were incubated for 20 min at 37 °C with gentle agitation in Ca^{2+}/Mg^{2+}-free HBSS plus 2′,7′-dichlorodihydrofluorescein diacetate. Subsequently, the cells were centrifuged at 1600 rpm for 10 min (room temperature), washed with HBSS, and centrifuged again using the same settings. After resuspension in HBSS at 5×10^6 cells/ml with anacardic acid, CNSE anacardic acid, salicylic acid, or PMA with or without the ROS scavenger DPI, cells (100 μl) were either added to a 96-well assay plate to assess fluorescence intensity using a SpectraMax M3 plate reader (485-nm excitation, and 530-nm emission) or 12×75-mm tubes for analysis on a FACSCalibur cell analyzer (BD Biosciences). To quantify extracellular ROS, the cells were seeded in black plates at a density of 2×10^5 cells/well in the presence of 10 μM lucigenin (Sigma-Aldrich) prior to the addition of anacardic acid or PMA. ROS release was determined via quantification of luminescence on an EnSpire Plate reader (PerkinElmer Life Sciences) using the standard luminescence protocol.

Quantification of LL-37 Release—Neutrophils were seeded in a 24-well plate at a density of 1×10^6 cells/well in HBSS with

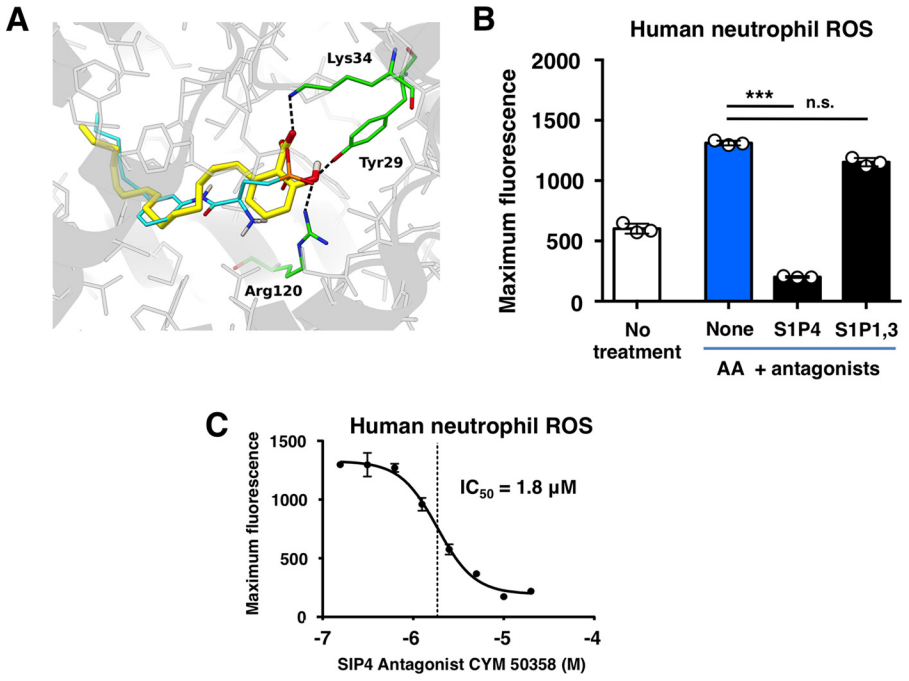

FIGURE 5. **Anacardic acid stimulates neutrophils via the S1P4 S1PR.** *A*, docking of anacardic acid to the S1PR (Protein Data Bank code 3V2Y). The sphingolipid mimic present in the crystal structure is highlighted in *yellow*, and anacardic acid is highlighted in *green/white*. Anacardic acid binds to the binding pocket with a binding affinity of −10.03 kcal/mol. The aliphatic 15-carbon tail fills the large hydrophobic pocket, and the head group contains conserved hydrogen bonds to S1P1 residues Tyr[29], Lys[34], and Arg[120]. *B*, ROS production in response to anacardic acid in the presence of antagonists of the S1P4-selective antagonist CYM50358 or the S1P1/3 antagonist VPC23019 (both 10 μM). *C*, concentration-response curve showing the effect of CYM50358 on anacardic acid-induced ROS production. The data shown are expressed as mean values ± S.D. and a representative experiment is shown of at least three independent experiments performed in triplicate. Where applicable, the results were analyzed by one-way analysis of variance and post hoc Newman Keuls test. ***, $p < 0.001$ *versus* control values.

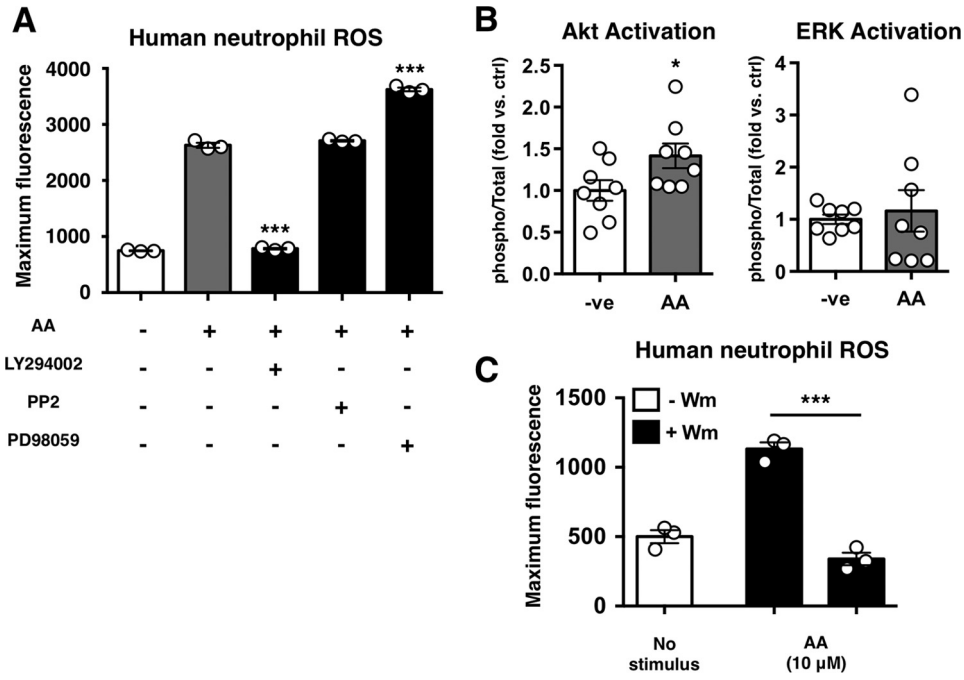

FIGURE 6. **Anacardic acid signals through PI3K.** *A*, anacardic acid stimulated ROS production in the presence of inhibitors of PI3K (LY294002; 10 μM), Src (PP2; 100 nM), or MEK (PD98059; 50 μM). Representative experiment is shown of three independent experiments performed in triplicate. *B*, results of total/phospho-Akt/ERK ELISAs showing fold change in the total/phospho-Akt/ERK ratio *versus* control ($n = 8$). *C*, anacardic acid- and PMA-stimulated ROS production in the presence of the PI3K inhibitor wortmannin (*Wm;* 10 μM) ($n = 3$). Unless otherwise noted, data shown are expressed as mean values ± S.E. of at least three independent experiments. Where applicable, the results were analyzed by one-way analysis of variance and post hoc Newman Keuls test. *, $p < 0.05$; ***, $p < 0.001$ *versus* control values.

Ca^{2+}/Mg^{2+}. The cells were then spun for 5 min at 400 × *g*. Following addition of anacardic acid or PMA, cells were incubated for 30–60 min at 37 °C with 5% CO_2. Supernatant samples (3 μl) were then collected and spotted on a nitrocellulose membrane, which was blocked in PBST with 5% fat-free milk for 1 h, washed three times with PBS, and incubated using an LL-37 (1:1000) anti-

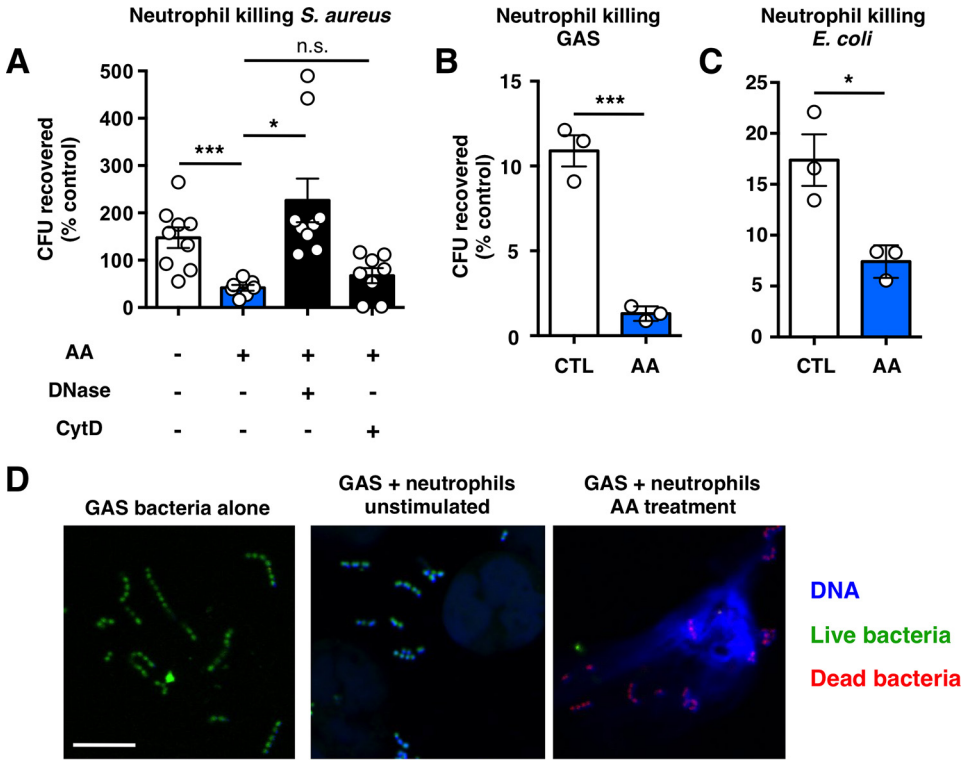

FIGURE 7. **Anacardic acid enhances bacterial killing.** *A*, neutrophil killing of USA300 MRSA. Control represents bacteria exposed to unstimulated neutrophils and anacardic acid represents neutrophils treated with 10 μM anacardic acid. DNase (7.5 units/ml) or cytochalasin D (10 μg/ml) were added to inhibit NET- or phagocytosis-based killing, respectively ($n = 9$). *B* and *C*, neutrophil killing of group A *Streptococcus* (*B*) and *E. coli* (*C*) by unstimulated or anacardic acid-treated (*AA*; 10 μM) neutrophils; representative experiments of three independent experiments performed in triplicate are shown. *D*, confocal microscopy visualization of live/dead (green/red) stained group A *Streptococcus* in the presence of human neutrophils stimulated with anacardic acid (10 μM). The *scale bar* represents 10 μm. Unless otherwise noted, data shown are expressed as mean values ± S.E. and represent the results of at least three independent experiments performed in triplicate. Where applicable, the results were analyzed by one-way analysis of variance and post hoc Newman Keuls test. ***, $p < 0.001$ *versus* control values. *ctrl*, control.

body overnight (Santa Cruz Biotechnology). Following three washes, the cells were incubated with a horseradish peroxidase secondary antibody for 1 h prior to membrane development.

Total/phospho-Akt/Erk ELISA. Relative levels of total/phospho-Akt/Erk were determined using InstantOne ELISA kits (eBiosciences, San Diego, CA) according to the manufacturer's protocol, with minor modifications. The cells were seeded at a density of 2×10^5 cells/well in HBSS + 5% FBS (total volume, 20 μl) and allowed to equilibrate for 1 h. Anacardic acid, PMA, or HBSS was then added (20 μl of 2× stock) to applicable wells, and the cells were incubated for 1 h at 37 °C with 5% CO_2. The cells were then lysed in lysis buffer provided by the manufacturer with the addition of 50 μl/ml 50× protease inhibitor mixture (cOmplete Protease Inhibitor Mixture Tablets; Roche). Subsequent steps were performed as directed in the manufacturer's protocol, and absorbance at 450 nm was performed using EnSpire Plate reader (PerkinElmer Life Sciences). The ratio of total/phospho-Akt and -ERK was determined for all treatment groups and plotted as fold change above untreated control samples.

Immunocytochemistry of gp91^{phox}—Neutrophils were seeded in Nunc LabTek 8-well chambered coverglass slides (Thermo Fisher Scientific) at a density of 2×10^5 cells/well. Following addition of 10 μM anacardic acid or vehicle control (HBSS), the cells were incubated for indicated times at 37 °C with 5% CO_2 prior to the addition of 16% paraformaldehyde (4% final concentration). Following 1 h of block/permeabilization in 2% BSA-PBS with 2% normal goat serum and 0.25% Triton X-100, fixed cells were washed three times with PBS prior to incubation for 1 h with an anti-NOX2/gp91^{phox} antibody (1 μg/ml in 2% BSA-PBS; Abcam; product no. ab80508). The cells were then washed three times with PBS prior to incubation with an Alexa Fluor 488-conjugated goat anti-rabbit secondary antibody (1:500; Thermo Fisher Scientific) for 1 h in 2% BSA-PBS. Following an additional three washes in PBS, the cells were incubated for 10 min with 1 mM Hoechst-33342-trihydrochloride to stain nuclei. Images were obtained using a Zeiss AxioObserver D1 microscope equipped with a plan Apochromat 63×/1.4 objective.

NET-based Bacterial Killing Assay—Neutrophils in RPMI + 2% 70 °C heat-inactivated FBS were added to a 24-well plate at a density of 4×10^5 cells/well with or without anacardic acid. After a 4-h incubation at 37 °C (with 5% CO_2), 4×10^4 bacteria were added to each well (multiplicity of infection of 0.1), and plates were spun at 1600 rpm for 5 min. After an additional 15-min incubation at 37 °C (with 5% CO_2), supernatant samples were serially diluted in 96-well plates containing sterile H_2O and plated on Todd Hewitt broth agar plates to determine percentage survival *versus* inoculum.

FRET-based PKC Activity Assay—HeLa cells were plated on sterilized glass coverslips in 35-mm dishes in DME containing 10% FBS. The cells were cultured at 37 °C with 5% CO_2 and upon reaching 60–80% confluency were transfected with CKAR, a FRET-based reporter for PKC-mediated phosphorylation, using jetPRIME (Polyplus-transfection). Following a

24-h incubation at 37 °C with 5% CO_2, the cells were washed with HBSS (Cellgro) containing 1 mM $CaCl_2$ prior to imaging on a Zeiss Axiovert microscope. To assess PKC activation levels, anacardic acid was added to cells, and cyan fluorescent protein, yellow fluorescent protein, and FRET images were acquired and used to calculate the average FRET ratio as previously described (27). Following the addition of anacardic acid, phorbol 12,13-dibutyrate, a PKC activator, was added as a positive control.

SUMOylation Assay—Neutrophils were seeded in 24-well plates in serum-free RPMI with or without anacardic acid. After 2 h, the cells were washed twice with PBS and lysed using radioimmune precipitation assay lysis buffer (150 mM NaCl, 50 mM Tris, pH 7.4, 5 mM EDTA, 1% Nonidet P-40, and 1% deoxcholic acid supplemented with protease inhibitor (Roche Applied Science). The BCA assay (Thermo Scientific) was used to determine the protein concentration. Equal amounts of total protein were loaded and separated on 10% or 6% SDS-polyacrylamide gels and transferred to a nitrocellulose membrane (Bio-Rad). The membranes were blocked with 5% nonfat milk and washed in Tris-buffered saline with 0.1% Tween 20 (TBST) twice for 5 min each. The membranes were subsequently incubated with SUMO-2/3 primary antibody (1:200 in TBST; Life Technologies; product no. 51-9100) at 1 μg/ml in 5% BSA/TBST. Following overnight incubation at 4°C, the membranes were washed and treated with a HRP-conjugated secondary antibody (Cell Signaling Technology, Danvers, MA) for 1 h at room temperature. Signals were detected by enhanced chemiluminescence (PerkinElmer Life Sciences) and exposed on Kodak BioMax light film.

Docking—AutoDockTools (version 1.5.6) (28) was used to generate input files for docking. The receptor structure (Protein Data Bank code 3V2Y) was prepared by removing non-standard residues, adding hydrogens and charges, and generating the PDBQT file. Anacardic acid three-dimensional coordinates have been generated from SMILES string using OpenBabel (29), and then AutoDockTools was used to add charges, merge non-polar hydrogens, set rotatable bonds, and generate the PDBQT. A cubic box of 70 points (26.25 Å side) was approximately centered on the crystallographic ligand (x, 5.220; y, 17.347; and z, −9.225), and docking was performed using Autodock 4.2.5.1. Default Lamarckian genetic algorithm settings were used, generating 1000 poses, which have been clustered using 2.0 Å, RMSD, and the lowest energy pose was selected to be analyzed.

Statistical Analysis—All statistical analyses described in the figure legends were performed using GraphPad Prism version 5.0.

Author Contributions—G. B. K., B. G. N., and J. J. P. P. provided critical reagents and inspired the initial analysis of immune boosting properties of anacardic acid. A. H., R. C., and V. N. designed the experiments. A. H., R. C., G. G., S. D., J. O., S. R. A., and A. L. performed the experiments. M. T. K. and A. C. N. designed and conducted the FRET-based PKC activity assay and associated signaling studies. S. F. and J. J. P. P. performed the *in silico* docking studies of receptor-ligand interactions. A. H., R. C., and V. N. wrote the paper, and all authors reviewed the manuscript and provided critical input.

References

1. World Health Organization (2014) Antimicrobial Resistance: Global Report on Surveillance, WHO Press, World Health Organization, Geneva, Switzerland
2. Newman, D. J., Cragg, G. M., and Snader, K. M. (2003) Natural products as sources of new drugs over the period 1981–2002. *J. Nat. Prod* **66,** 1022–1037
3. Hemshekhar, M., Sebastin Santhosh, M., Kemparaju, K., and Girish, K. S. (2012) Emerging roles of anacardic acid and its derivatives: a pharmacological overview. *Basic Clin. Pharmacol. Toxicol.* **110,** 122–132
4. Mamidyala, S. K., Ramu, S., Huang, J. X., Robertson, A. A., and Cooper, M. A. (2013) Efficient synthesis of anacardic acid analogues and their antibacterial activities. *Bioorg. Med. Chem. Lett.* **23,** 1667–1670
5. Seong, Y., Shin, P.-G., Yoon, J.-S., Yadunandam, A. K., and Kim, G.-D. (2014) Induction of the endoplasmic reticulum stress and autophagy in human lung carcinoma A549 cells by anacardic acid. *Cell Biochem. Biophys.* **68,** 369–377
6. Kubo, J., Lee, J. R., and Kubo, I. (1999) Anti-*Helicobacter pylori* agents from the cashew apple. *J. Agric. Food Chem.* **47,** 533–537
7. Sharma, R., Kishore, N., Hussein, A., and Lall, N. (2013) Antibacterial and anti-inflammatory effects of *Syzygium jambos* L. (Alston) and isolated compounds on acne vulgaris. *BMC Complement Altern. Med.* **13,** 292
8. Balasubramanyam, K., Swaminathan, V., Ranganathan, A., and Kundu, T. K. (2003) Small molecule modulators of histone acetyltransferase p300. *J. Biol. Chem.* **278,** 19134–19140
9. Sung, B., Pandey, M. K., Ahn, K. S., Yi, T., Chaturvedi, M. M., Liu, M., and Aggarwal, B. B. (2008) Anacardic acid (6-nonadecyl salicylic acid), an inhibitor of histone acetyltransferase, suppresses expression of nuclear factor-κB–regulated gene products involved in cell survival, proliferation, invasion, and inflammation through inhibition of the inhibitory subunit of nuclear factor-$\kappa B\alpha$ kinase, leading to potentiation of apoptosis. *Blood* **111,** 4880–4891
10. Omanakuttan, A., Nambiar, J., Harris, R. M., Bose, C., Pandurangan, N., Varghese, R. K., Kumar, G. B., Tainer, J. A., Banerji, A., Perry, J. J., and Nair, B. G. (2012) Anacardic acid inhibits the catalytic activity of matrix metalloproteinase-2 and matrix metalloproteinase-9. *Mol. Pharmacol.* **82,** 614–622
11. Pietrocola, F., Lachkar, S., Enot, D. P., Niso-Santano, M., Bravo-San Pedro, J. M., Sica, V., Izzo, V., Maiuri, M. C., Madeo, F., Mariño, G., and Kroemer, G. (2015) Spermidine induces autophagy by inhibiting the acetyltransferase EP300. *Cell Death Differ.* **22,** 509–516
12. Harsha Raj, M., Yashaswini, B., Rössler, J., and Salimath, B. P. (2016) Combinatorial treatment with anacardic acid followed by TRAIL augments induction of apoptosis in TRAIL resistant cancer cells by the regulation of p53, MAPK and NF$\kappa\beta$ pathways. *Apoptosis* **21,** 578–593
13. Trevisan, M. T., Pfundstein, B., Haubner, R., Würtele, G., Spiegelhalder, B., Bartsch, H., and Owen, R. W. (2006) Characterization of alkyl phenols in cashew (*Anacardium occidentale*) products and assay of their antioxidant capacity. *Food Chem. Toxicol.* **44,** 188–197
14. Melo Cavalcante, A. A., Rubensam, G., Picada, J. N., Gomes da Silva, E., Fonseca Moreira, J. C., and Henriques, J. A. (2003) Mutagenicity, antioxidant potential, and antimutagenic activity against hydrogen peroxide of cashew (*Anacardium occidentale*) apple juice and cajuina. *Environ. Mol. Mutagen.* **41,** 360–369
15. Pandey, D., Chen, F., Patel, A., Wang, C.-Y., Dimitropoulou, C., Patel, V. S., Rudic, R. D., Stepp, D. W., and Fulton, D. J. (2011) SUMO1 Negatively regulates reactive oxygen species production from NADPH oxidases. *Arterioscler. Thromb. Vasc. Biol.* **31,** 1634–1642
16. Brinkmann, V., Reichard, U., Goosmann, C., Fauler, B., Uhlemann, Y., Weiss, D. S., Weinrauch, Y., and Zychlinsky, A. (2004) Neutrophil extracellular traps kill bacteria. *Science* **303,** 1532–1535
17. Keiser, M. J., Roth, B. L., Armbruster, B. N., Ernsberger, P., Irwin, J. J., and Shoichet, B. K. (2007) Relating protein pharmacology by ligand chemistry. *Nat. Biotechnol.* **25,** 197–206
18. von Köckritz-Blickwede, M., and Nizet, V. (2009) Innate immunity turned inside-out: antimicrobial defense by phagocyte extracellular traps. *J. Mol. Med.* **87,** 775–783
19. Wartha, F., and Henriques-Normark, B. (2008) ETosis: A novel cell death pathway. *Sci. Signal.* **1,** pe25
20. Corriden, R., Hollands, A., Olson, J., Derieux, J., Lopez, J., Chang, J. T., Gonzalez, D. J., and Nizet, V. (2015) Tamoxifen augments the innate immune function of neutrophils through modulation of intracellular ceramide. *Nat. Commun.* **6,** 8369

21. Guerrero, M., Urbano, M., Velaparthi, S., Zhao, J., Schaeffer, M. T., Brown, S., Rosen, H., and Roberts, E. (2011) Discovery, design and synthesis of the first reported potent and selective sphingosine-1-phosphate 4 (S1P4) receptor antagonists. *Bioorg. Med. Chem. Lett.* **21,** 3632–3636
22. Kihara, Y., Mizuno, H., and Chun, J. (2015) Lysophospholipid receptors in drug discovery. *Exp. Cell Res.* **333,** 171–177
23. Allende, M. L., Bektas, M., Lee, B. G., Bonifacino, E., Kang, J., Tuymetova, G., Chen, W., Saba, J. D., and Proia, R. L. (2011) Sphingosine-1-phosphate lyase deficiency produces a pro-inflammatory response while impairing neutrophil trafficking. *J. Biol. Chem.* **286,** 7348–7358
24. Rada, B., Jendrysik, M. A., Pang, L., Hayes, C. P., Yoo, D.-G., Park, J. J., Moskowitz, S. M., Malech, H. L., and Leto, T. L. (2013) Pyocyanin-enhanced neutrophil extracellular trap formation requires the NADPH oxidase. *PLoS One* **8,** e54205
25. Gräler, M. H., Grosse, R., Kusch, A., Kremmer, E., Gudermann, T., and Lipp, M. (2003) The sphingosine 1-phosphate receptor S1P4 regulates cell shape and motility via coupling to G_i and $G_{12/13}$. *J. Cell. Biochem.* **89,** 507–519
26. Lappano, R., and Maggiolini, M. (2011) G protein-coupled receptors: novel targets for drug discovery in cancer. *Nat. Rev. Drug Discov.* **10,** 47–60
27. Violin, J. D., Zhang, J., Tsien, R. Y., and Newton, A. C. (2003) A genetically encoded fluorescent reporter reveals oscillatory phosphorylation by protein kinase C. *J. Cell Biol.* **161,** 899–909
28. Morris, G. M., Huey, R., Lindstrom, W., Sanner, M. F., Belew, R. K., Goodsell, D. S., and Olson, A. J. (2009) AutoDock4 and AutoDockTools4: Automated docking with selective receptor flexibility. *J. Comput. Chem.* **30,** 2785–2791
29. O'Boyle, N. M., Banck, M., James, C. A., Morley, C., Vandermeersch, T., and Hutchison, G. R. (2011) Open Babel: An open chemical toolbox. *J. Cheminform.* **3,** 33